AGU PUBLICATIONS

Geophysical Research Letters

RESEARCH LETTER
10.1002/2017GL073801

Key Points:
- Developed a new algorithm to estimate magnitudes of large earthquakes
- Applied this approach to $M_w \geq 7.0$ earthquakes from 2004 to 2014
- Propose to build an automated system for fast estimates of magnitude and source length of large earthquakes

Supporting Information:
- Supporting Information S1
- Figures S1–S7 and Tables S1 and S2

Correspondence to:
D. Wang,
dunwang2004@yahoo.com

Citation:
Wang, D., H. Kawakatsu, J. Zhuang, J. Mori, T. Maeda, H. Tsuruoka, and X. Zhao (2017), Automated determination of magnitude and source length of large earthquakes using backprojection and *P* wave amplitudes, *Geophys. Res. Lett.*, *44*, 5447–5456, doi:10.1002/2017GL073801.

Received 28 JUN 2016
Accepted 23 MAY 2017
Accepted article online 30 MAY 2017
Published online 12 JUN 2017

Automated determination of magnitude and source length of large earthquakes using backprojection and *P* wave amplitudes

Dun Wang[1,2], Hitoshi Kawakatsu[2], Jiancang Zhuang[3], Jim Mori[4], Takuto Maeda[2], Hiroshi Tsuruoka[2], and Xu Zhao[5]

[1]State Key Laboratory of Geological Processes and Mineral Resources, School of Earth Sciences, China University of Geosciences, Wuhan, China, [2]Earthquake Research Institute, University of Tokyo, Tokyo, Japan, [3]Institute of Statistical Mathematics, Tachikawa, Japan, [4]Disaster Prevention Research Institute, Kyoto University, Kyoto, Japan, [5]Institute of Geology and Geophysics, China Academy of Sciences, Beijing, China

Abstract Fast estimates of magnitude and source extent of large earthquakes are fundamental for disaster mitigation. However, resolving these estimates within 10–20 min after origin time remains challenging. Here we propose a robust algorithm to resolve magnitude and source length of large earthquakes using seismic data recorded by regional arrays and global stations. We estimate source length and source duration by backprojecting seismic array data. Then the source duration and the maximum amplitude of the teleseismic *P* wave displacement waveforms are used jointly to estimate magnitude. We apply this method to 74 shallow earthquakes that occurred within epicentral distances of 30–85° to Hi-net (2004–2014). The estimated magnitudes are similar to moment magnitudes estimated from W-phase inversions (U.S. Geological Survey), with standard deviations of 0.14–0.19 depending on the global station distributions. Application of this method to multiple regional seismic arrays could benefit tsunami warning systems and emergency response to large global earthquakes.

1. Introduction

Rapid determination of earthquake magnitude is important for estimating the potential for shaking damage and tsunami hazard. However, because of the complexity of source processes, accurate estimations of the magnitudes of great earthquakes within minutes after origin time remain a challenge. For example, for the first few hours following the 2004 M_w 9.1 Sumatra earthquake, seismologists had underestimated its magnitude as 8.2–8.5 [*Park et al.*, 2005]. Another example is the 2011 M_w 9.0 Tohoku, Japan earthquake, the magnitude of which was underestimated significantly as *M* 7.9 for the first 30 min after the origin time, resulting in the fatal delay of tsunami evacuation in many areas along the east coast of Japan [*Hayes et al.*, 2011].

Local (Richter) magnitude M_L, body wave magnitude m_b, surface wave magnitude M_s, and moment magnitude M_w are four basic magnitude scales commonly used today for measuring earthquake sizes. For $M >= 8.0$ earthquakes, the former three magnitude scales become saturated, causing severe underestimation of earthquake size. The M_w scale does not become saturated for earthquakes of any size; therefore, it can provide an accurate estimate of the size of a large earthquake. However, estimating M_w requires entire wave trains including *P*, *S*, and surface waves, which takes tens of minutes to reach seismic stations at teleseismic distances. As body waves are the first signals to arrive at these stations, they are used for the rapid determination of moment magnitude in several newly developed seismic moment inversion methods. For example, the National Earthquake Information Center of the U.S. Geological Survey (USGS) implements an automated fast moment tensor inversion using body waves, which estimates moment magnitudes within 30 min after origin time. Another approach that can offer promising estimate of M_w is W-phase inversion [*Duputel et al.*, 2011; *Kanamori and Rivera*, 2008]. Hereafter, all references to M_w mean the moment magnitude estimated by W-phase inversion (M_{ww}).

In addition to methods that involve inversions, other approaches use empirical relations to estimate earthquake magnitudes, usually for large earthquakes [e.g., *Convers and Newman*, 2013; *Hara,* 2007a; *Katsumata et al.*, 2013; *Lomax and Michelini*, 2009; *Noda et al.*, 2016; *Tsuboi et al.*, 1995, 1999]. Their simple implementation and straightforward calculation made these approaches widely applied by many institutions such as the Pacific Tsunami Warning Center, Japan Meteorological Agency, and USGS.

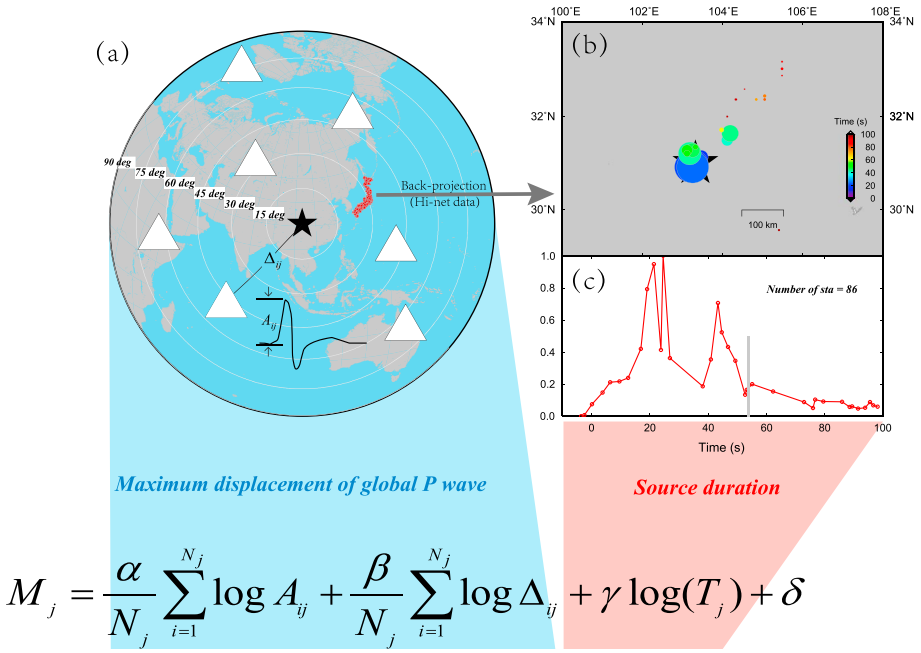

Figure 1. Methodology for determining magnitudes of large earthquakes. Magnitude is estimated by combining (a) maximum displacements of global *P* wave amplitudes and (c) source durations. Here the source duration is estimated by backprojection analyses using a large regional seismic array. The grid line in Figure 1c shows the cutoff where the rupture ends. (b) Color circles indicate the local maximums of the stacked energies. Here A_{ij} is the maximum vertical displacement of the teleseismic *P* wave recorded at the *i*th station for event *j*, and Δ_{ij} is the epicenter distance (km). Parameter T_j is the source duration derived from the backprojections, and *N* is the number of global stations. The operator log denotes the decimal logarithm.

Here we develop an approach derived from the method of *Hara* [2007a] for estimating earthquake magnitudes by considering *P* wave displacements and source durations (Figure 1). In *Hara* [2007a], source duration was approximated empirically from the envelope of high-frequency waveforms recorded at teleseismic distances. A good azimuthal coverage and short scattered coda waves that are generated around stations are generally desired for correct estimation of source duration. We introduce a backprojection technique [*Wang et al.*, 2016b] instead to estimate source duration using array data from the high-sensitivity seismograph network (Hi-net) of the National Research Institute for Earth Science and Disaster Prevention (NIED) in Japan [*Okada et al.*, 2004]. Backprojection has been proven efficient at resolving rupture durations and source extents of large seismic sources [*Fan and Shearer*, 2015; *Honda and Aoi*, 2009; *Ishii et al.*, 2005; *Kennett et al.*, 2014; *Koper et al.*, 2012; *Krüger and Ohrnberger*, 2005; *Meng et al.*, 2011; *Okuwaki et al.*, 2014; *Wang et al.*, 2016b; *Yao et al.*, 2011; *Zhang et al.*, 2011].

The introduction of backprojection improves the method in two ways. First, the source duration can be determined accurately by seismic arrays. The duration of envelopes of high-frequency waves are affected frequently by possibly strong site effects and directivity effects at global stations. Therefore, many stations with uniform azimuthal distribution were required to acquire good estimates of earthquake magnitudes in *Hara* [2007a]. The backprojection method inherently accounts for directivity effects and minimizes the coda waves generated at individual array stations. Second, the results can be calculated more rapidly. We find that earthquake magnitudes can be constrained well using determined source durations and a few nearby stations, meaning data derived from distant stations are not always required.

In this study we propose a reliable algorithm for determining fast and reliable source information of large shallow seismic events based on real-time data of a dense regional array and global data, for earthquakes that occur at a distance of roughly 30–85° from the array center. The time required for the estimation is largely attributable to the traveltime from the hypocenter to the array stations; therefore, we can obtain results within 6–13 min (plus source duration time) depending on the epicenter distance. This system can offer fast and robust estimates of the magnitudes and the rupture lengths for large earthquakes. It could prove a

promising aid for disaster mitigation immediately following a damaging earthquake, especially when dealing with the tsunami evacuation and emergency response.

2. Methodology

This approach is intended to obtain earthquake source information including magnitude, source length, and high-frequency energy distribution quickly (within 6–13 min in addition to source duration time) after the occurrence of a large earthquake 30–85° from the center of a large regional array. The procedure includes two principal steps: (1) backprojection of waveforms recorded by the regional array and (2) global distribution of *P* wave amplitudes.

The backprojection results provide estimates of the spatial source length and the source duration in time. Combining this source duration with the global *P* wave amplitudes provides the estimate of earthquake magnitude.

2.1. Backprojection

We backproject waveforms recorded by a large array to obtain the spatial and temporal distribution of the energy release within the source area, using the method described in *Wang et al.* [2016b].

The procedure consists of the following steps.

1. Retrieve real-time *P* wave waveforms recorded at the vertical component of each station from the data center of the seismic array.
2. Remove mean, baseline correction, and tapering.
3. Set up a horizontal grid of 60 × 60 points at the depth of the hypocenter, covering an area 3 times that of the source area as estimated by a scaling law [*Wells and Coppersmith*, 1994], according to the magnitude in an earthquake catalog.
4. Align and cross-correlate waveforms to calculate station corrections (e.g., Figure S1 in the supporting information). The cross correlation is performed between a model waveform recorded around the center of the array and the other stations. Two frequency bands of 0.05–0.30 and 0.5–2.0 Hz are used for this analysis, and the lengths of the stacking windows are 20 and 6 s, respectively. Noisy data are eliminated if the correlation coefficient with the reference waveform is less than 0.4 for both frequency bands. The number of stations is reduced by setting a minimum distance of 50 km between stations.
5. Perform a backprojection analysis [*Wang et al.*, 2016b] with the following settings, band-pass filter: 0.5–2.0 Hz; window length: 10 s; and interval between windows: 2 s. Traveltimes are calculated in advance and stored on a local server using the IASPEI91 model of *Kennett and Engdahl* [1991].

The backprojection results provide an accurate estimate of rupture length and an energy-time plot, as shown in the example of Figure 1. The value of the source duration used for the magnitude estimation is determined based on the energy-time plot of the backprojection results. For each earthquake, we estimate a duration, for which 90% of the stacked energy has been included, and another duration, for which the amplitude of the stacked energy is smaller than 0.1 time the maximum stacked energy and 80% of the stacked energy has been included. We define the shorter of the two durations as the source duration. We compare our determined source durations (Figure S2 and Table S1) with those obtained by W-phase inversion [*Duputel et al.*, 2013], Global centroid moment tensor (CMT) inversion [*Ekström and Nettles*, 2015], and energy duration [*Convers and Newman*, 2013] (Figure 2). Notice that the source durations derived from W-phase inversion and Global CMT inversion are approximated by 2 times of the centroid time delays [*Duputel et al.*, 2013]. Source durations determined by the backprojections are similar to those determined by the W-phase and Global CMT inversions. However, for the 2004 giant Sumatra earthquake, our approach estimates the source duration as lasting as 472 s. This is consistent with other studies using different methods [*Lay et al.*, 2005; *Ni et al.*, 2005], and it is 2 times the durations estimated by the W-phase and Global CMT inversions. On average, the energy durations are longer than our determined duration by a factor of 1.5. Further investigation of these discrepancies among them would help better understanding of the complexities of seismic sources and improve the accuracy of magnitude determination.

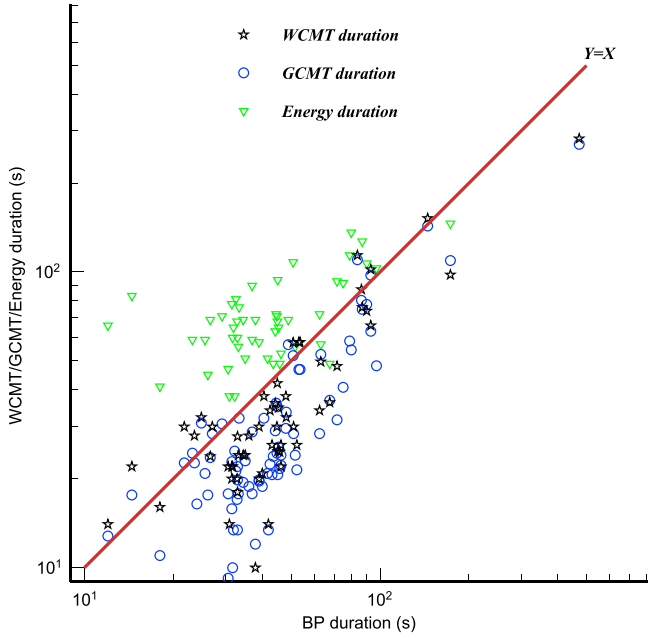

Figure 2. Comparisons of source durations derived from the backprojections in this study with W-phase inversion durations by *Duputel et al.* [2013] (earthquakes 2004–2012), Global CMT inversion durations by *Ekström and Nettles* [2015] (earthquakes 2004–2014), and energy durations by *Convers and Newman* [2013] (earthquakes April 2007–2014).

2.2. Global Distribution of *P* Wave Amplitudes

We download data from the global seismic stations of the Incorporated Research Institutions for Seismology (IRIS) located within 10–85° with respect to the earthquake epicenters. First, we remove the instrument response and then calculate the maximum displacement for the waveforms from the theoretically estimated *P* arrival time to *S* arrival time. The plot of *P* wave amplitudes as a function of epicentral distance reveals a different trend for the data from 10 to 40° compared with 40 to 85° (Figure S3). Therefore, when using the amplitudes to compute the magnitude, we use two sets of parameters for the two distance ranges.

2.3. Estimating Magnitude

As the coda waves generated at individual Hi-net stations are minimized at the source time function after stacking in the backprojection, the duration of the coherent high-frequency waves represents the source duration, as has been shown in many case studies [e.g., *Ishii et al.*, 2005; *Krüger and Ohrnberger*, 2005].

We estimate the magnitude of seismic events by combining the maximum displacements of the teleseismic *P* waves and the source durations derived from backprojection (Figures S2 and S3). Motivated by *Hara* [2007b], we develop an equation as

$$\begin{aligned} K^1 &= 0.53\sum_{i=1}^{N_1}\log A_i + 0.44\sum_{i=1}^{N_1}\log\Delta_i + 1.01\log(\text{duration}) + 6.23 \\ K^2 &= 0.51\sum_{i=1}^{N_2}\log A_i - 0.01\sum_{i=1}^{N_2}\log\Delta_i + 1.05\log(\text{duration}) + 7.89\,, \\ M_{\text{dt}} &= \frac{N_1{}^{*}K^1 + N_2{}^{*}K^2}{N_1 + N_2} \end{aligned} \tag{1}$$

where A_i is the maximum vertical displacement of the teleseismic *P* wave recorded at the *i*th station, and Δ_i is the epicenter distance (km). Parameters N_1 and N_2 represent the number of stations with epicenter distances of 10–40 and 40–85°, respectively. Throughout this paper, the operator log denotes the decimal logarithm. Notice that the coefficients for the LogA and Log (duration) are estimated using data in Figures S2 and S3, which are detailed in section 3.1.2.

The magnitude is estimated by the maximum displacement (*D*) of the *P* waves and source time duration (*T*); therefore, to distinguish it from M_w, hereafter we call it M_{dt}.

3. Results for Large Shallow Earthquakes (2004–2014)

We systematically test this approach for earthquakes that occurred from 2004 to 2014 with shallow depths (up to 60 km). In order to test the applicability of this method fully, we apply the algorithm for

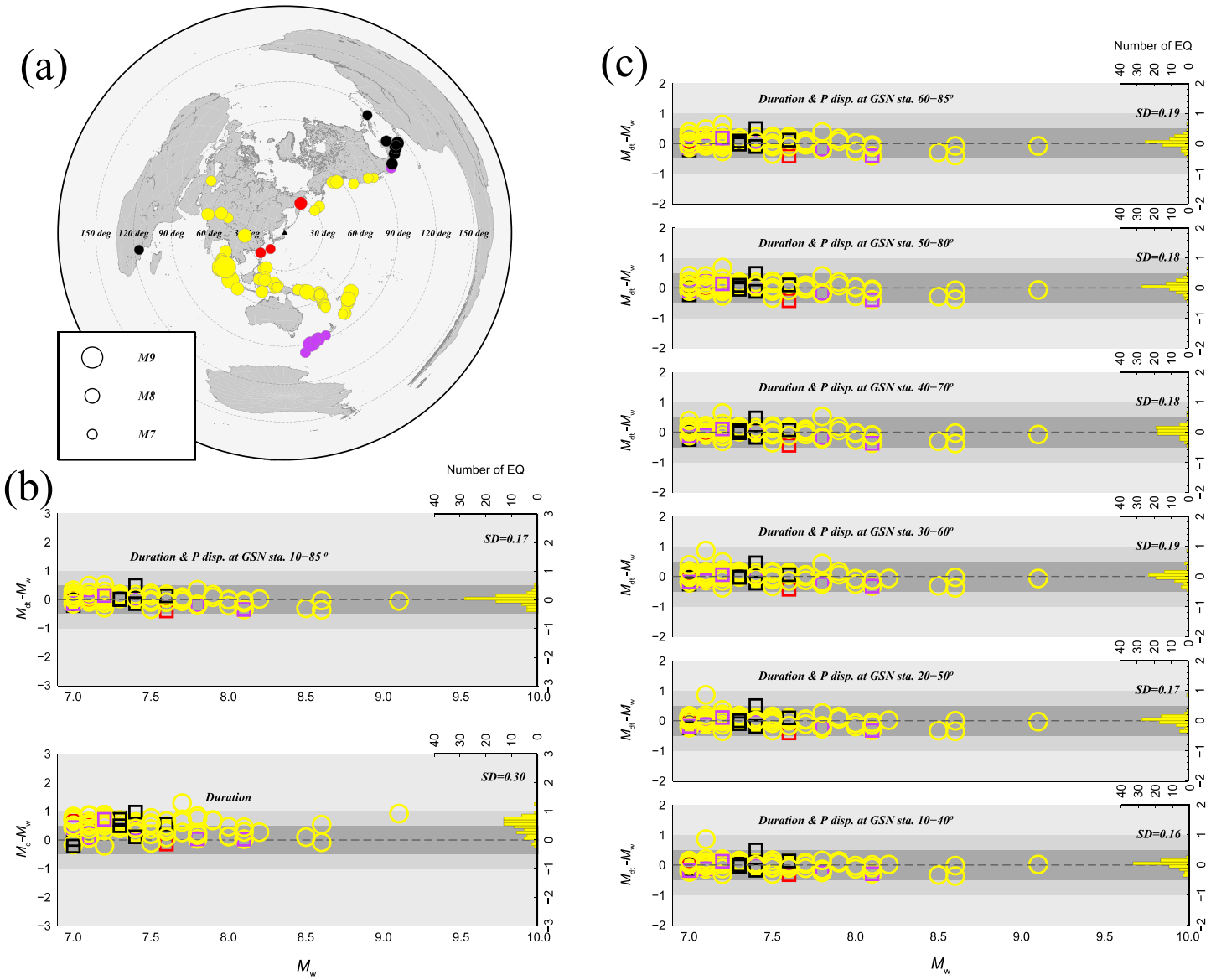

Figure 3. (a) Locations of earthquakes analyzed in this study. Dashed lines represent the distances to the Hi-net center (black triangle). Color indicates the distance ranges to the Hi-net center (red, 15–30; yellow, 30–85; purple, 85–100; black, 100–120°). (b) (top) Comparison of M_w (USGS) and our estimates (M_{dt}) derived from the source duration and maximum P wave amplitudes of global stations located at 15–120° from the epicenters. Color indicates distance ranges to the Hi-net center. Inset histogram shows the frequency content of the differences of magnitudes between M_w (USGS) and M_{dt} for earthquakes that are 30–85° to the Hi-net center. Number at the top right shows the standard deviation. (bottom) Same as Figure 3b (top) but for magnitudes estimated from source duration (M_d). (c) Comparison of M_w (USGS) and our estimates (M_{dt}) derived from source duration and maximum displacement of global stations at a series of distance ranges from the epicenters. Notice that the parameters used in equation (4) for estimating M_{dt} are the same as in the Figure 3b (top).

earthquakes that satisfy the following criteria in the USGS catalog: Depth $\leq$ 60 km, $M_w \geq$ 7.0, and Distance (to station N.HMNH) of 15–120°. Although precise rupture patterns for earthquakes with magnitudes as small as 7.0–7.5 are difficult to resolve by backprojection, we want to assess how the magnitude determination component of this method works for earthquakes that reach the lower magnitude threshold. Similarly, earthquakes that are too close to or too far from the Hi-net array are also included in this analysis.

Figure 3a shows the locations of the 93 earthquakes included in this analysis. Most earthquakes were located along the Sumatra arc, Cascadia, and California, covering regions where large historical damaging earthquakes and/or tsunamis have occurred.

3.1. Estimating Magnitude

The estimated magnitudes for the 93 earthquakes are compared to M_w (USGS). Figure 3b shows the difference between M_{dt} and M_w for the 93 earthquakes. It shows that M_{dt} is a reasonable estimate of M_w and that the difference has a standard deviation of 0.17 for 74 earthquakes that are 30–85° to the Hi-net center.

3.1.1. Duration Magnitude

We show the difference between a duration magnitude M_d and M_w, to demonstrate the improvement achieved by adding the global *P* wave amplitudes in relation to using just the source duration. Following *Ekström et al.* [1992], the seismic moment can be calculated from the source duration estimated by backprojection via

$$M_0 = \left(0.5\times10^8\times T\right)^3. \tag{2}$$

We convert this moment to a magnitude (M_d) using [*Hanks and Kanamori*, 1979]

$$M_d = \left(\frac{\log M_0}{1.5}\right) - 10.73, \tag{3}$$

which is compared with M_w in Figure 3b (bottom). The differences of M_d and M_w show a scatter that is larger than the differences of M_{dt} and M_w, as seen in the histogram shown on the right of Figure 3b. The results show large scatter (>0.5) for earthquakes with magnitude less than 7.5. For great earthquakes ($M_w \geq 8.0$), the uncertainties are mostly less than 0.3 after proper correction, suggesting that source duration might be appropriate for approximate evaluation of the magnitudes of large earthquakes. However, the 2004 M_w 9.1 Sumatra earthquake was an extreme case that had very long duration, which makes its duration magnitude equal to 10.

3.1.2. Magnitude Determined by Duration and Maximum Displacement

Combining source duration and maximum displacement of *P* waves can offer better estimates for large earthquakes. We first use an empirical formula [*Hara*, 2007a] of

$$M_j = \frac{\alpha}{N_j}\sum_{i=1}^{N_j}\log A_{ij} + \frac{\beta}{N_j}\sum_{i=1}^{N_j}\log\Delta_{ij} + \gamma\log\left(T_j\right) + \delta, \tag{4}$$

where M_j is the magnitude of the *j*th event; A_{ij} is the maximum amplitude of the displacement of the *P* wave at the *i*th station, with a distance of Δ_{ij}; N_j is the number of stations involved in the estimation of M_j; and α, β, γ, and δ are parameters to be estimated. Using data from all stations for epicenter distances between 10 and 85° for the 74 earthquakes, we fit the parameters α, β, γ, and δ as 0.55, 0.67, 1.01, and 5.55, respectively. Our results suggest that most estimates (M_{dt}) for earthquakes with distance range of 30–85° from the Hi-net array agree well with the USGS estimates, with a standard deviation of 0.17, although the deviations for $M_w \leq 7.5$ earthquakes are larger (Figure 3b, top).

As this method is designed for automated real-time determination of the magnitudes of large earthquakes, we investigate how the global station distribution affects the final estimates. Using the parameters estimated above (for equation (4)) and global stations located at different distance ranges for calculating the maximum displacements of the *P* waves, we find the overall estimates are not affected greatly by the distance range of global stations (Figure 3c), suggesting that this approach is robust and that it does not require the inclusion of data from many global stations. Furthermore, data from the closest station range appear slightly better at constraining the results than the data derived from more distant stations (Figure 3c), except for an aftershock (2013/02/06 01:23 *M* 7.1) of the 2013 M_w 8.0 Solomon earthquake (2013/02/06 01:12), for which the *P* wave maximum displacements were distorted by the surface waveforms of the main shock. These tests suggest that our method can issue reliable and robust estimates under various circumstances with different distributions of global stations.

We use global data at a series of distance ranges to fit the parameters in equation (4) and find that more global data do not produce better results than using data from stations within a narrow distance interval (Table S2). The best estimation model (standard deviation 0.14) is obtained by choosing records within the epicenter distance interval of [10, 40)°, where parameters α, β, γ, and δ are 0.53, 0.44, 1.01, and 6.23,

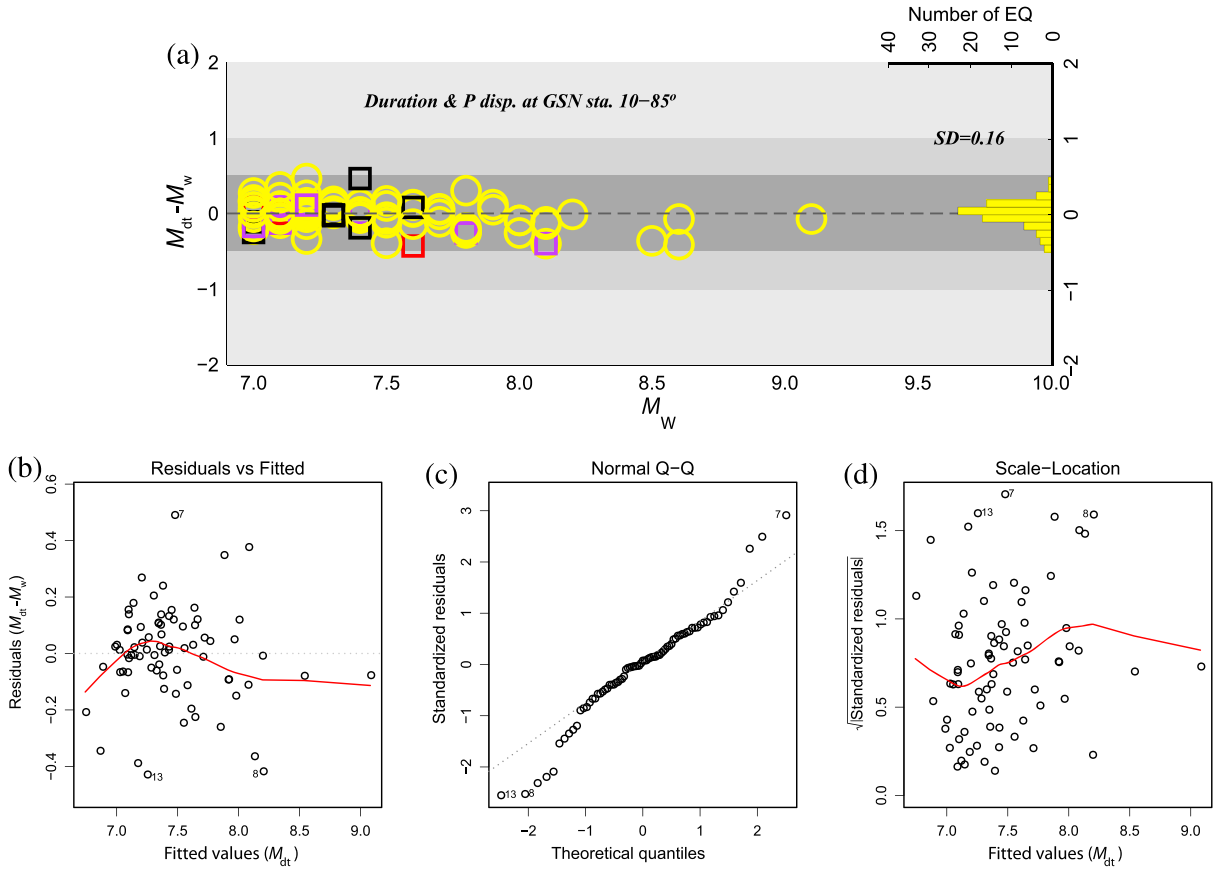

Figure 4. (a) Comparison of M_w (USGS) and M_{dt} derived from the source duration and maximum *P* wave displacements of GSN stations that are 15–120° from the epicenters using equation (1). Color indicates distance ranges to the Hi-net center (same as Figure 3a). (b) Residuals as function of determined magnitudes, providing overall evaluation of the trend. (c) Normal quantile-quantile plot, used to verify whether residuals belong to a normal distribution. The horizontal axis gives the theoretical quantiles of the standard normal distribution, and the vertical axis gives the corresponding quantiles of the standardized residuals. (d) Scale-location plot of sqrt(|residuals|) as a function of determined values (M_{dt}).

respectively. These parameters are 0.51, −0.01, 1.05, and 7.89, when using data from the epicenter distance interval of [40, 85)°. In the latter case, the epicenter distance in equation (4) has almost no contribution to the estimation of M_{dt} because the maximum amplitudes of the *P* wave displacements do not vary in this epicentral distance range. This is because the relation among the magnitude, *P* wave amplitude, and epicenter-station distance is not simply linear or log linear. For example, the *P* wave amplitude decreases with epicenter distance of 10 to 40°, but it remains constant or decrease slightly over 40° (Figure S3). To account for this feature and to pursue optimal equations for the estimations, we use equation (1) instead of a single set of parameters (e.g., equation (4)), to estimate the magnitudes. The two sets of designed distance ranges are 10–40 and 40–85°. As shown in Figure 4, the new model shows smaller standard deviation of 0.16, which can be reduced to 0.14 if only the closest global stations (10–40° to epicenters) are used. Even for a special case of the 2006 *M* 7.7 Java tsunami earthquake with long source duration, the magnitude is accurately estimated.

To evaluate the magnitude variations with elapsed time, we mimic a real-time environment to determine the magnitudes of all the earthquakes using equation (1) (Figure S4). The determined magnitudes show slight variation (within ±0.2 on average), except for the event (2013/02/06 *M* 7.1) whose maximum displacements of direct *P* waves were contaminated by the main shock.

3.2. Source Length

Case studies suggest that backprojections using a dense regional array are capable of resolving source length and high-frequency energy radiations of earthquakes with magnitudes larger than or equal to about M_w 7.5

[*Fan and Shearer*, 2015; *Ishii et al.*, 2005; *Kennett et al.*, 2014; *Koper et al.*, 2012; *Krüger and Ohrnberger*, 2005; *Wang et al.*, 2016a]. It is difficult to accurately resolve rupture areas of major to large earthquakes due to the effect of array smear [*Wang et al.*, 2016c]. Here we compare the source lengths of the 74 earthquakes derived from the backprojections with an empirically determined magnitude-length relationship [*Wells and Coppersmith*, 1994]. The source lengths are determined by measuring the maximum distances from the epicenter to the backprojected source locations with normalized amplitudes of equal or larger than 0.3. Notice that the amplitude threshold used here for measuring duration is higher than the one used for determining duration, because the spatial locations of the backprojected sources become highly unstable when the normalized amplitudes drop to 0.3 or smaller. Using the source lengths derived in this study, we obtain a scaling relationship between magnitude and source length (Figure S5), which is $\log(L) = -2.614 + 0.619^{*}\mathrm{Mag}$. The standard deviation is 0.4, which is 2 to 3 times larger than the standard deviations of the magnitude estimations in section 3.1. The large uncertainties are probably caused by the reduced numbers of seismic stations, resolution of the backprojection method, or variation of the stress drops at the fault planes.

The source lengths are not constrained well in this study, but the fault layouts and the high-frequency energy radiation areas appear accurate for $M_w \geq 7.5$ earthquakes, as confirmed by several well-studied cases such as the 2013 M_w 7.7 Pakistan earthquake [*Avouac et al.*, 2014; *Wang et al.*, 2016a]. Our backprojection results show the rupture migrated to the southwest (Figure S6), which is confirmed by coseismic surface displacements [*Avouac et al.*, 2014].

4. Timing

We have shown that the magnitude and energy release of large earthquakes can be accurately determined jointly using a regional array and global data. As the calculations are relatively simple, this process could be operated automatically, and it could generate results in near-real time. The time required by this system is largely attributable to the traveltime of the *P* waves from the hypocenter to the regional array. The maximum displacement of the *P* wave can be estimated quickly based on a few teleseismic observations with relatively close epicenter distances. We show in Figure 3c that there is little distance dependence for global *P* wave amplitude data. For shallow ($\leq$ 60 km) earthquakes, stations located 10, 30, and 90° from the epicenter will receive *P* waves at around 3, 6, and 13 min after origin time, respectively. For an earthquake that occurs at 30° to a regional array, this system could issue estimate of the magnitude and distribution of energy release within 6 min (plus source duration time). This would constitute one of the fastest issuances of reliable results for earthquake source size and length, which could be applied to tsunami estimation, and emergency response.

5. Discussion

By combining global and regional array data, both the magnitude and the source length of a large shallow seismic event can be determined automatically in near-real time. One limitation is that backprojection results are not as reliable for distance greater than 85°. Furthermore, for such earthquakes, it takes longer for the *P* wave train to arrive. Hence, multiple regional dense arrays around the world are necessary for monitoring global earthquakes. Currently, there are a handful of regional networks that are available for this purpose, such as the dense broadband stations in Europe, China, Australia, and the U.S. With multiple dense stations, response times could be minimized. For example, the China Array can determine source information within 10 min for large earthquakes (with source duration of less than 4 min) that occur in and around Japan, while it would take an additional 6 min if U.S. data are used because the greater distance requires more time for the direct *P* waves to arrive.

Our method uses data observed at regional to teleseismic distances, which is different from other methods adopted for the purpose of earthquake early warning using local seismic data [e.g., *Allen and Kanamori*, 2003; *Katsumata et al.*, 2013; *Noda et al.*, 2016; *Wu and Teng*, 2002]. Seismic waves at local distance often drive broadband seismometers off scale, which can be avoided at regional to teleseismic distances.

As mentioned in section 1, there was an underestimation problem in estimating the magnitude of the 2011 M_w 9.0 Tohoku earthquake. The magnitude was estimated as *M* 7.9 within the first 30 min. However, 34 min after the origin time, the USGS issued a magnitude of M_w 8.9 for this event based on W-phase inversion. By

applying our method to the data recorded at a series of distance ranges by the China Array (http://www.ceic.ac.cn/), we determine a magnitude of M_{dt} = 8.8–9.1, which is a reasonably good estimate in comparison with other studies [*Duputel et al.*, 2011; *Hara*, 2011; *Hayes*, 2011; *Nettles et al.*, 2011; *Shao et al.*, 2011]. Considering the short distance from the epicenter to the array (Figure S7), the results could have been produced within 6–10 min after the origin time. Other methods, such as the real-time W-phase inversion, require 20 min after the origin time, although the response time could be expected to reduce to 7 min using regional data [*Duputel et al.*, 2011].

6. Conclusions

We proposed an algorithm that can automatically determine both the magnitude (M_{dt}) and source length of large shallow earthquakes in near-real time using real-time seismic data recorded by a large regional array, such as Hi-net in Japan, in conjunction with *P* wave amplitudes from global stations. We applied this method to 74 earthquakes that occurred between 2004 and 2014 (M_w 7.0 to M_w 9.2) within 30–85° of Hi-net. The magnitudes were estimated well with standard deviations of 0.14–0.19, depending on the distributions of the global stations used in calculating the maximum displacement amplitudes of the *P* waves. As the results could be produced within 6–13 min (plus the source duration time), this system could be useful for rapid tsunami estimation, shaking damage prediction, and possible practical implementation of emergency response strategies.

Acknowledgments
This work was supported by the fellowship of the Japan Society for the Promotion of Science (P13324), National Natural Science Foundation of China grants 41004020 and 41474050, and the Fundamental Research Funds for the Central Universities (CUG170602), China University of Geosciences (Wuhan) (D.W.). Hi-net data were obtained from the NIED. Other data were obtained from the IRIS Data Center, USGS website, and Global CMT website. This work benefited from discussions and comments from Tatsuhiko Hara, Seiji Tsuboi, Shiro Ohmi, Hiroe Miyake, Kazushige Obara, and Aitaro Kato. We sincerely thank the Editor Andrew V. Newman and two anonymous reviewers for their constructive comments. All the figures were created using the Generic Mapping Tools (GMT) of Wessel and Smith [*Wessel and Smith*, 1991].

References

Allen, R., and H. Kanamori (2003), The potential for earthquake early warning in Southern California, *Science*, *300*(5620), 786–789.
Avouac, J.-P., F. Ayoub, S. Wei, J.-P. Ampuero, L. Meng, S. Leprince, R. Jolivet, Z. Duputel, and D. Helmberger (2014), The 2013, M_w 7.7 Balochistan earthquake, energetic strike-slip reactivation of a thrust fault, *Earth Planet. Sci. Lett.*, *391*, 128–134.
Convers, J. A., and A. V. Newman (2013), Rapid earthquake rupture duration estimates from teleseismic energy rates, with application to real-time warning, *Geophys. Res. Lett.*, *40*, 5844–5848, doi:10.1002/2013GL057664.
Duputel, Z., L. Rivera, H. Kanamori, G. P. Hayes, B. Hirshorn, and S. Weinstein (2011), Real-time W phase inversion during the 2011 off the Pacific coast of Tohoku earthquake, *Earth Planets Space*, *63*(7), 535–539.
Duputel, Z., V. C. Tsai, L. Rivera, and H. Kanamori (2013), Using centroid time-delays to characterize source durations and identify earthquakes with unique characteristics, *Earth Planet. Sci. Lett.*, *374*, 92–100.
Ekström, G., and M. Nettles (2015), *Long-Period Moment-Tensor Inversion: The Global CMT Project*, pp. 1360–1371, Springer, Berlin, Heidelberg.
Ekström, G., R. S. Stein, J. Eaton, and D. Eberhart-Phillips (1992), Seismicity and geometry of a 110-km-long blind thrust fault 1. The 1985 Kettleman Hills, California, earthquake, *J. Geophys. Res.*, *97*(B4), 4843–4864, doi:10.1029/91JB02925.
Fan, W., and P. M. Shearer (2015), Detailed rupture imaging of the 25 April 2015 Nepal earthquake using teleseismic *P* waves, *Geophys. Res. Lett.*, *42*, 7467–7475, doi:10.1002/2015GL064587.
Hanks, T. C., and H. Kanamori (1979), A moment magnitude scale, *J. Geophys. Res.*, *84*(B5), 2348–2350, doi:10.1029/JB084iB05p02348.
Hara, T. (2007a), Magnitude determination using duration of high frequency energy radiation and displacement amplitude: Application to tsunami earthquakes, *Earth Planets Space*, *59*(6), 561–565.
Hara, T. (2007b), Measurement of the duration of high-frequency energy radiation and its application to determination of the magnitudes of large shallow earthquakes, *Earth Planets Space*, *59*(4), 227–231.
Hara, T. (2011), Magnitude determination using duration of high frequency energy radiation and displacement amplitude: Application to the 2011 off the Pacific coast of Tohoku earthquake, *Earth Planets Space*, *63*(7), 525–528.
Hayes, G. P. (2011), Rapid source characterization of the 2011 M_w 9.0 off the Pacific coast of Tohoku earthquake, *Earth Planets Space*, *63*(7), 529–534.
Hayes, G. P., P. S. Earle, H. M. Benz, D. J. Wald, and R. W. Briggs (2011), 88 hours: The U.S. Geological Survey National Earthquake Information Center response to the 11 March 2011 M_w 9.0 Tohoku earthquake, *Seismol. Res. Lett.*, *82*(4), 481–493.
Honda, R., and S. Aoi (2009), Array back-projection imaging of the 2007 Niigataken Chuetsu-oki earthquake striking the world's largest nuclear power plant, *Bull. Seismol. Soc. Am.*, *99*(1), 141–147.
Ishii, M., P. M. Shearer, H. Houston, and J. E. Vidale (2005), Extent, duration and speed of the 2004 Sumatra-Andaman earthquake imaged by the Hi-Net array, *Nature*, *435*(7044), 933–936, doi:10.1038/Nature03675.
Kanamori, H., and L. Rivera (2008), Source inversion of W phase: Speeding up seismic tsunami warning, *Geophys. J. Int.*, *175*(1), 222–238.
Katsumata, A., H. Ueno, S. Aoki, Y. Yoshida, and S. Barrientos (2013), Rapid magnitude determination from peak amplitudes at local stations, *Earth Planets Space*, *65*(8), 843–853.
Kennett, B., and E. Engdahl (1991), Traveltimes for global earthquake location and phase identification, *Geophys. J. Int.*, *105*(2), 429–465.
Kennett, B., A. Gorbatov, and S. Spiliopoulos (2014), Tracking high-frequency seismic source evolution: 2004 M_w 8.1 Macquarie event, *Geophys. Res. Lett.*, *41*, 1187–1193, doi:10.1002/2013GL058935.
Koper, K. D., A. R. Hutko, T. Lay, and O. Sufri (2012), Imaging short-period seismic radiation from the 27 February 2010 Chile (M_w 8.8) earthquake by back-projection of *P*, *PP*, and *PKIKP* waves, *J. Geophys. Res.*, *117*, B02308, doi:10.1029/2011JB008576.
Krüger, F., and M. Ohrnberger (2005), Tracking the rupture of the M_w=9.3 Sumatra earthquake over 1,150 km at teleseismic distance, *Nature*, *435*(7044), 937–939, doi:10.1038/Nature03696.
Lay, T., H. Kanamori, C. J. Ammon, M. Nettles, S. N. Ward, R. C. Aster, S. L. Beck, S. L. Bilek, M. R. Brudzinski, and R. Butler (2005), The great Sumatra-Andaman earthquake of 26 December 2004, *Science*, *308*(5725), 1127–1133.
Lomax, A., and A. Michelini (2009), Mwpd: A duration-amplitude procedure for rapid determination of earthquake magnitude and tsunamigenic potential from *P* waveforms, *Geophys. J. Int.*, *176*(1), 200–214.

Meng, L., A. Inbal, and J. P. Ampuero (2011), A window into the complexity of the dynamic rupture of the 2011 M_w 9 Tohoku-Oki earthquake, *Geophys. Res. Lett.*, *38*, L00G07, doi:10.1029/2011GL048118.

Nettles, M., G. Ekström, and H. C. Koss (2011), Centroid-moment-tensor analysis of the 2011 off the Pacific coast of Tohoku earthquake and its larger foreshocks and aftershocks, *Earth Planets Space*, *63*(7), 519–523.

Ni, S., H. Kanamori, and D. Helmberger (2005), Seismology: Energy radiation from the Sumatra earthquake, *Nature*, *434*(7033), 582–582.

Noda, S., S. Yamamoto, and W. L. Ellsworth (2016), Rapid estimation of earthquake magnitude from the arrival time of the peak high-frequency amplitude, *Bull. Seismol. Soc. Am.*, *106*(1), 232–241.

Okada, Y., K. Kasahara, S. Hori, K. Obara, S. Sekiguchi, H. Fujiwara, and A. Yamamoto (2004), Recent progress of seismic observation networks in Japan-Hi-net, F-net, K-NET and KiK-net, *Earth Planets Space*, *56*(8), 15–28.

Okuwaki, R., Y. Yagi, and S. Hirano (2014), Relationship between high-frequency radiation and asperity ruptures, revealed by hybrid back-projection with a non-planar fault model, *Sci. Rep.*, *4*.

Park, J., R. Butler, K. Anderson, J. Berger, P. Davis, H. Benz, C. R. Hutt, C. S. McCreery, T. Ahern, and G. Ekström (2005), Performance review of the global seismographic network for the Sumatra-Andaman megathrust earthquake, *Seismol. Res. Lett.*, *76*(3), 331–343.

Shao, G., X. Li, C. Ji, and T. Maeda (2011), Focal mechanism and slip history of the 2011 M_w 9.1 off the Pacific coast of Tohoku earthquake, constrained with teleseismic body and surface waves, *Earth Planets Space*, *63*(7), 559–564.

Tsuboi, S., K. Abe, K. Takano, and Y. Yamanaka (1995), Rapid determination of M_w from broadband *P* waveforms, *Bull. Seismol. Soc. Am.*, *85*(2), 606–613.

Tsuboi, S., P. M. Whitmore, and T. J. Sokolowski (1999), Application of Mwp to deep and teleseismic earthquakes, *Bull. Seismol. Soc. Am.*, *89*(5), 1345–1351.

Wang, D., H. Kawakatsu, J. Mori, B. Ali, Z. Ren, and X. Shen (2016a), Backprojection analyses from four regional arrays for rupture over a curved dipping fault: The M_w 7.7 24 September 2013 Pakistan earthquake, *J. Geophys. Res. Solid Earth*, *121*, 1948–1961, doi:10.1002/2015JB012168.

Wang, D., J. Mori, and K. Koketsu (2016b), Fast rupture propagation for large strike-slip earthquakes, *Earth Planet. Sci. Lett.*, *440*, 115–126.

Wang, D., N. Takeuchi, H. Kawakatsu, and J. Mori (2016c), Estimating high frequency energy radiation of large earthquakes by image deconvolution back-projection, *Earth Planet. Sci. Lett.*, *449*, 155–163.

Wells, D. L., and K. J. Coppersmith (1994), New empirical relationships among magnitude, rupture length, rupture width, rupture area, and surface displacement, *Bull. Seismol. Soc. Am.*, *84*(4), 974–1002.

Wessel, P., and W. H. Smith (1991), Free software helps map and display data, Eos, *EOS Trans. AGU*, *72*(41), 441–446.

Wu, Y.-M., and T.-l. Teng (2002), A virtual subnetwork approach to earthquake early warning, *Bull. Seismol. Soc. Am.*, *92*(5), 2008–2018.

Yao, H., P. Gerstoft, P. M. Shearer, and C. Mecklenbräuker (2011), Compressive sensing of the Tohoku-Oki M_w 9.0 earthquake: Frequency-dependent rupture modes, *Geophys. Res. Lett.*, *38*, L20310, doi:10.1029/2011GL049223.

Zhang, H., Z. Ge, and L. Ding (2011), Three sub-events composing the 2011 off the Pacific coast of Tohoku earthquake (M_w 9.0) inferred from rupture imaging by back-projecting teleseismic *P* waves, *Earth Planets Space*, *63*(7), 595–598.